

Robert Turner Carr

---

PHYSICAL BASIS FOR GAMMA-RAY SCIN-  
TILLATION DOSIMETRY.

Thesis  
C2716

Library  
U. S. Naval Postgraduate School  
Monterey, California

# PHYSICAL BASIS FOR GAMMA-RAY SCINTILLATION

## DOSIMETRY\*

Accurate roentgen measurements can be performed effectively with small scintillation crystals. Theoretical and experimental results are given for energies in the  $\gamma$ -ray region. The precautions necessary to obtain accurate data with organic scintillators are discussed.

by

R. T. Carr† and G. J. Hine‡

Department of Physics and Radioactivity Center of the  
Laboratory for Nuclear Science, Massachusetts Institute  
of Technology, Cambridge, Massachusetts

\*This work has been supported in part by the joint program of the ONR and AEC, and also in part by the Bureau of Ordnance, U. S. Navy.

†Now on sea duty, U. S. Navy. Investigation performed while a U. S. naval postgraduate student at Massachusetts Institute of Technology, Cambridge, Massachusetts.

‡From Radioisotope Unit, Veterans Administration Hospital, Boston, Massachusetts.

*Note: Not a Thesis, but the by-product of  
Thesis research. Prepared for publication  
in Nucleonics.*

Thesis

C2716

Dosage measurements obtained with air ionization chambers can be expressed in roentgen units. For other types of detectors to have a response also expressible in roentgens, their x- or  $\gamma$ -ray energy absorption must be proportional to that of air. Under certain conditions organic scintillators exhibit such a behaviour (1).

Several investigators (1, 2, 3) have studied the energy dependence of anthracene crystals for x-rays with energies below 250 kv. In the present investigation the energy range is expanded up to about 3 Mev using  $\gamma$ -ray emitters. In addition the effect of scintillator thickness, secondary electron equilibrium, and scattered radiation have been studied.

### Theoretical Considerations

In order to determine the air equivalent energy range for scintillation materials, calculations of the ratio of the energy absorbed per sec in the scintillation material, I, to the energy absorbed per sec in air, D, are made. For true air equivalence, I/D must be independent of the incident  $\gamma$ -ray energy.

The energy absorbed per sec,  $dE_T$ , for an incident  $\gamma$ -ray flux of  $n$  photons/cm<sup>2</sup>-sec in a material of thickness  $dx$  and area  $A$  is

$$dE_T = nA \left[ \sigma_a E_\gamma + \tau E_\gamma + \kappa (E_\gamma - 2m_0 c^2) \right] dx \quad (1)$$



where

$E_\gamma$  =  $\gamma$ -ray energy in Mev

$\sigma_a$  = "true" Compton absorption coefficient in  $\text{cm}^{-1}$

$\tau$  = photoelectric attenuation coefficient in  $\text{cm}^{-1}$

$\kappa$  = pair-production attenuation coefficient in  $\text{cm}^{-1}$

For organic scintillators and  $\gamma$ -ray energies  $E_\gamma < 10$  Mev

$$\kappa(E_\gamma - 2m_0c^2) \ll \sigma_a E_\gamma$$

and therefore

$$dE_T \cong nAE_\gamma [\sigma_a + \tau] dx = nAE_\gamma \mu_a dx \quad (2)$$

where

$$\mu_a = \sigma_a + \tau$$

If  $n_0$  is the number of photons/ $\text{cm}^2$ -sec incident on the surface of the material, the number of photons present at any depth,  $x$  cm inside the material, is given by

$$n = n_0 e^{-\mu_0 x} \quad (3)$$

where  $\mu_0 = \sigma_a + \sigma_s + \tau + \kappa$ . The total linear attenuation coefficient is used here since the probability of multiple scattering is small within a few grams of scintillation material.

The total energy absorbed per sec in a medium of thickness  $h$  and volume  $(Ah)$  follows from Eqs. (2) and (3) as:





$$E_T = \int_0^h \left( \frac{dE_T}{dx} \right) dx = n_o \mu_a E_\gamma h A \left[ \frac{1 - e^{-\mu_o h}}{\mu_o h} \right] \quad (4)$$

Finally the ratio, I/D, of the energy absorbed per sec in an organic scintillator to that in air follows as

$$\frac{I}{D} = \frac{E_T(\text{scint.})}{E_T'(\text{air})} = \frac{\mu_a}{\mu_a'} \frac{hA}{h'A'} \frac{\left[ \frac{1 - e^{-\mu_o h}}{\mu_o h} \right]}{\left[ \frac{1 - e^{-\mu_o' h'}}{\mu_o' h'} \right]} \quad (5)$$

where the primes refer to air. Equation (5) expresses the energy dependence of scintillation materials relative to that of air for  $\gamma$  rays of various energies. Under experimental conditions the  $\gamma$ -ray absorption in air-wall ionization chambers is small and the ratio  $\frac{hA}{h'A'}$  is constant. Therefore I/D can be expressed as

$$\frac{I}{D} = C \frac{\mu_a}{\mu_a'} \left[ \frac{1 - e^{-\mu_o h}}{\mu_o h} \right] \quad (6)$$

Equation (6) is the final result for the energy response of scintillators in comparison with air for monochromatic  $\gamma$  rays. For  $\gamma$ -ray beams of various energies  $E_{\gamma_i}$  the ratio I/D becomes:

$$\frac{I}{D} = C \frac{\sum_i n_{o_i} \mu_{a_i} E_{\gamma_i} \left[ \frac{1 - e^{-\mu_{o_i} h}}{\mu_{o_i} h} \right]}{\sum_i n_{o_i} \mu_{a_i}' E_{\gamma_i}} \quad (7)$$

where  $(n_o)_i$  is the number of photons/cm<sup>2</sup>-sec of energy



$(E_\gamma)_1$  incident on the surface of the detector.

For anthracene crystals of various thickness,  $I/D$  given in Eq. (6) has been evaluated as a function of the energy of the incident  $\gamma$  rays. Curve A in Fig. 1 shows the results for a very thin crystal of thickness  $h = 0$ . The attenuation coefficients used for these calculations were obtained from recent NBS computations (4). The constant,  $C$ , is chosen so that  $I/D$  equals unity for  $E_\gamma = 0.6$  Mev. For this energy,  $\tau$  is very small compared with  $\delta_a$ , and therefore the condition for air equivalence is fulfilled automatically. From curve A of Fig. 1 it follows that the energy chosen for normalization could have been selected anywhere between 0.2 and 2.0 Mev since in this interval  $I/D$  is linear and equal to unity. This energy interval is the true "air-equivalent" range for thin anthracene crystals.

Curves B and C in Fig. 1 show the results for anthracene crystals of thickness  $h = 6$  mm and  $h = 25$  mm respectively, both normalized at 0.6 Mev. The shape of curves B and C is similar to that for the zero thick crystal (curve A). However, for  $h = 6$  mm  $I/D$  is constant only for a narrow energy interval from 0.3 Mev to 0.8 Mev and for a thick crystal ( $h = 25$  mm)  $I/D$  varies continuously with the energy of the  $\gamma$  rays. This is caused by the fact that although the  $\gamma$ -ray absorption is negligible in the air medium the same is not true for the scintillator.



For dosage measurements for which an accuracy of about 5 percent is adequate, it appears from Fig. 1 that a few centimeters thick anthracene crystals may still be regarded as air-equivalent over a limited energy range.

The above discussion, concerning only anthracene, can be extended for other organic compounds such as stilbene, terphenyl, naphthalene, and others. In the energy range considered, the true absorption coefficient  $\mu_a$  is approximately equal to  $\sigma_a$  which varies with  $Z/A$ . For all light elements, except hydrogen,  $Z/A$  is essentially constant and therefore the results obtained for anthracene apply to most organic compounds.

#### Experimental Procedure

The instruments, an air ionization chamber, and a scintillation detector, are both employed as dose rate meters. The ionization chamber (3 mm thick bakelite cylinder, volume 1.6 liters) is part of a commercial Beckman Radioactivity Meter Model MX-4. The scintillation detector consists of one of several types of scintillation materials mounted on an RCA 5819 photomultiplier tube. The output of the photomultiplier is connected directly to an RCA WV-84A DC microammeter modified by inserting a feedback capacitance of 1.0 uf between the plate and grid of the input tube (2).

In order to minimize the amount of scattered radiation reaching the detectors, the ionization chamber and scintillation detector are mounted on an aluminum frame approximately 2



1

meters apart and 1.5 meters above a wooden table. The ceiling, walls, and floor are all at a distance greater than 2.5 meters from either detector or source. Even under these conditions it appeared that the amount of radiation scattered into the detectors was not negligible. In order to obtain results relevant to the outlined theoretical calculations all sources were placed in a lead collimator which reduced the contribution due to scattered radiation to a point where it was no longer detectable.

The experimental results obtained with a cylindrical anthracene crystal (diameter 30 mm, height  $h = 6$  mm) are shown in Fig. 2. The experimental data are normalized for the  $\text{Cs}^{137}$  measurement. The theoretical curve  $I/D$  for this anthracene crystal, normalized at 0.6 Mev, is replotted in Fig. 2. Excellent agreement with theory is observed for the  $\text{Hg}^{203}$ ,  $\text{Cs}^{137}$ , and  $\text{Co}^{60}$  data. The low value for the  $\text{Na}^{24}$   $\gamma$  rays results from the leakage of secondary electrons from the 6 mm thick crystal (5).

To our knowledge no previous experimental results are available in the  $\gamma$ -ray energy region. Experimental data obtained by Breitling with x-rays of energies below 250 Kvp are shown in Fig. 3. The experimental value obtained with the highest energy x-rays were plotted to coincide with the theoretical curve normalized at 0.6 Mev. Considering the difficulties encountered when working with low energy x-rays





and the possible contribution from scattered radiation, which will increase the uncertainty in x-ray energy, there is also good agreement between experimental and theoretical data.

### Secondary Electron Equilibrium

The average secondary electron energy in anthracene is approximately 1.0 Mev for the  $\gamma$  rays from  $\text{Na}^{24}$  (5). The maximum range in anthracene for electrons of this energy is 3 mm. Therefore, the secondary electrons initiated in the last 3 mm of the crystal have a finite chance of leaving the crystal before all their energy is absorbed. To compensate for this loss of secondary electrons a piece of bakelite 3 mm thick was placed on top of the 6 mm anthracene crystal previously covered only by a 1/4 mil aluminum foil and a thin cardboard light shield. The experimental results for the new arrangement are included in Fig. 2. The  $\text{Na}^{24}$  data are now also in good agreement with the theoretical prediction. Those secondary electrons produced in the bakelite which enter the front face of the crystal compensate for the secondary electrons leaving the crystal back side. For the  $\text{Na}^{24}$   $\gamma$  rays an increase in dosage intensity was observed as the thickness of the bakelite was increased from 0 to 3 mm. For thicknesses greater than 3 mm the intensity slowly decreased due to absorption of  $\gamma$  rays in the bakelite.

The maximum range of the secondary electrons in anthracene for the  $\text{Co}^{60}$   $\gamma$  rays is about 1.5 mm. Since the



cardboard light shield and aluminum foil are equivalent to about 1 mm of anthracene the addition of bakelite did not increase the observed intensity.

All experimental results described thus far have been obtained with a 6 mm thick anthracene crystal. The loss of secondary electrons by leakage depends on the crystal thickness as well as on the energy of the incident  $\gamma$  rays. Figure 4 shows the percentage loss of secondary electrons as a function of crystal size for the  $\text{Na}^{24}$   $\gamma$  rays. It shows, as expected, that if the volume from which electrons can leak out becomes small in comparison with the whole scintillator, the percentage loss becomes negligible. This curve was obtained using plastic scintillators of various thickness. The data for  $\text{Na}^{24}$  were compared with those from lower energy  $\gamma$ -ray sources for which the electron leakage is negligible.

#### Scattered Radiation

As mentioned above some contribution due to scattered radiation reaching the detector was observed when using uncollimated sources. The measurements of I/D were repeated now using uncollimated sources and the results are shown in Fig. 5. Since the 6 mm thick anthracene crystal is not truly air equivalent (Fig. 1) the change in average  $\gamma$ -ray energy (primary plus scattered radiation) will affect the I/D values in two ways. A reduction in average  $\gamma$ -ray energy will lower I/D for low energy  $\gamma$ -rays ( $\text{Hg}^{203}$ ,  $\text{I}^{131}$ ) and will



reduce leakage loss for high energy radiation ( $\text{Na}^{24}$ ). The  $\text{Cs}^{137}$ , Ra, and  $\text{Co}^{60}$  results remained unchanged since they lie within the air equivalent energy region and leakage loss is negligible for these sources with a 6 mm anthracene crystal.

### Sodium Iodide

The solid line in Fig. 6 shows the theoretical ratio  $I/D$  for a 25 mm NaI crystal. The theoretical curve has been normalized at 1.5 Mev since at this energy  $\gamma$  and  $K$  are much smaller than  $\sigma_a$ . The experimental points in Fig. 6 were obtained with uncollimated sources and normalized for the  $\text{Co}^{60}$  data. As expected the high photoelectric absorption of  $\gamma$  rays in NaI for  $\gamma$  rays with energies below 0.6 Mev give values of  $I/D$  much greater than unity. However for  $\gamma$  rays with energies between 0.6 and 2.0 Mev the value of  $I/D$  remains rather constant since  $\sigma_a$  predominates over  $\tau$  and  $K$ . Therefore in this limited energy interval NaI(Tl) crystals appear to be suitable for dosage measurements.

### Conclusions

$\gamma$ -ray dosage measurements can be performed with organic scintillators. Results having a high accuracy can be obtained for  $\gamma$  rays with energies between 0.2 and 3.0 Mev if several factors are considered. With increasing crystal thickness the absorption of the  $\gamma$  radiation in the scintillator becomes more important. Therefore the accuracy of dosage measurements with thick organic scintillators is limited. When measuring



$\gamma$ -ray sources with energies above 1.0 Mev the scintillator must be covered by a suitable amount of air equivalent material in order to maintain secondary electron equilibrium.

A mixture of scattered and primary radiation exhibits a lowered average  $\gamma$ -ray energy compared with that emitted from the source. Therefore the dose rate measured with a scintillator will be smaller than that determined with an ionization chamber for primary  $\gamma$  radiation with energies below 0.3 Mev. The dosage resulting from higher energy  $\gamma$  rays can be accurately measured with a thin scintillator as long as the conditions for secondary electron equilibrium are fulfilled.





### Bibliography

1. V. G. Breitling. Ueber die Wellenlaengenabhaengigkeit der Fluoreszenz Organischer Leuchtstoffe im Roentgengebiet, Z. angew. Phys. 4, 401 (1952)
2. W. B. Ittner III and M. Ter-Pogossian. "Air Equivalence" of Scintillation Materials, Nucleonics 10, No. 2, 48 (1952)
3. G. J. Brucker. Energy Dependence of Scintillating Crystals, Nucleonics 10, No. 11, 72 (1952)
4. G. R. White, X-ray Attenuation Coefficients from 10 Kev to 100 Mev, National Bureau of Standards Report 1008, (1952)
5. G. D. Prestwich, T. H. Colvin, and G. J. Hine. Average Energy of Secondary Electrons in Anthracene Due to Gamma-Irradiation, Phys. Rev. 87, 1030 (1952)



### Legends for Figures

Fig. 1. Calculated ratio of energy absorbed per sec in anthracene, I, to energy absorbed per sec in air, D, as a function of  $\gamma$ -ray energy. Consideration of  $\gamma$ -ray absorption gives results depending on crystal thickness. All curves have been normalized to unity at 0.6 Mev.

Fig. 2. I/D as a function of  $\gamma$ -ray energy. Solid line taken from Fig. 1 curve B for 6 mm thick anthracene crystal. Experimental data obtained with collimated  $\gamma$ -ray beams are normalized for the Cs<sup>137</sup> data. Covering the crystal with bakelite affects only the Na<sup>24</sup> value since for the high energy Na<sup>24</sup>  $\gamma$  rays secondary electron equilibrium was not yet established.

Fig. 3. I/D as a function of x-ray energy for a 3.7 mm thick anthracene crystal. Experimental data shown have been obtained by Breitling (1).

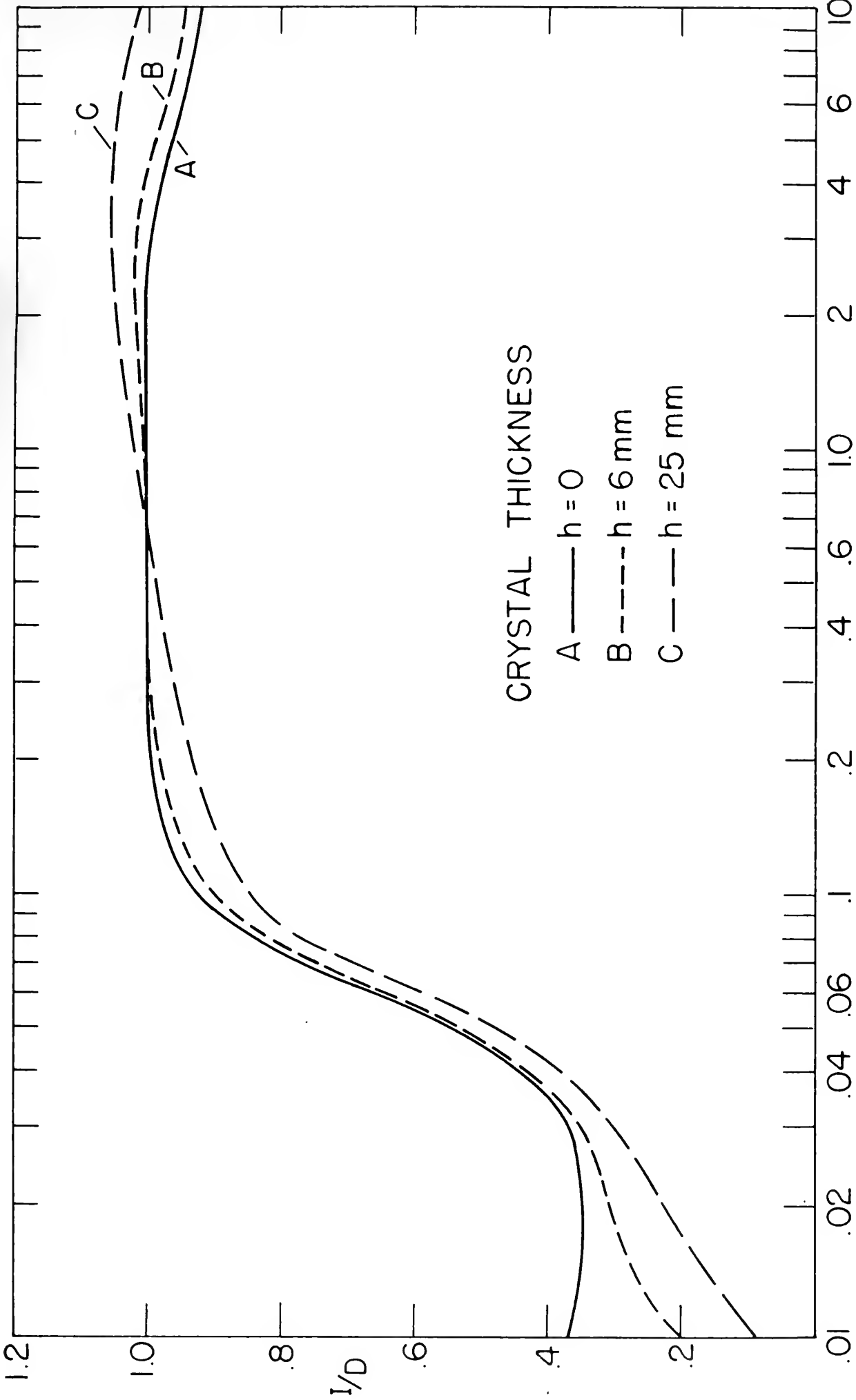
Fig. 4. Experimental data for the percentage loss of secondary electron energy produced by Na<sup>24</sup>  $\gamma$  rays in plastic scintillators. Scintillator diameter 2.6 cm, thickness ranging from 1.5 to 24 mm.

Fig. 5. I/D as a function of  $\gamma$ -ray energy for a 6 mm anthracene crystal. Experimental data obtained with uncollimated  $\gamma$ -ray beams. The contribution of scattered radiation appears to lower the average  $\gamma$ -ray energy.



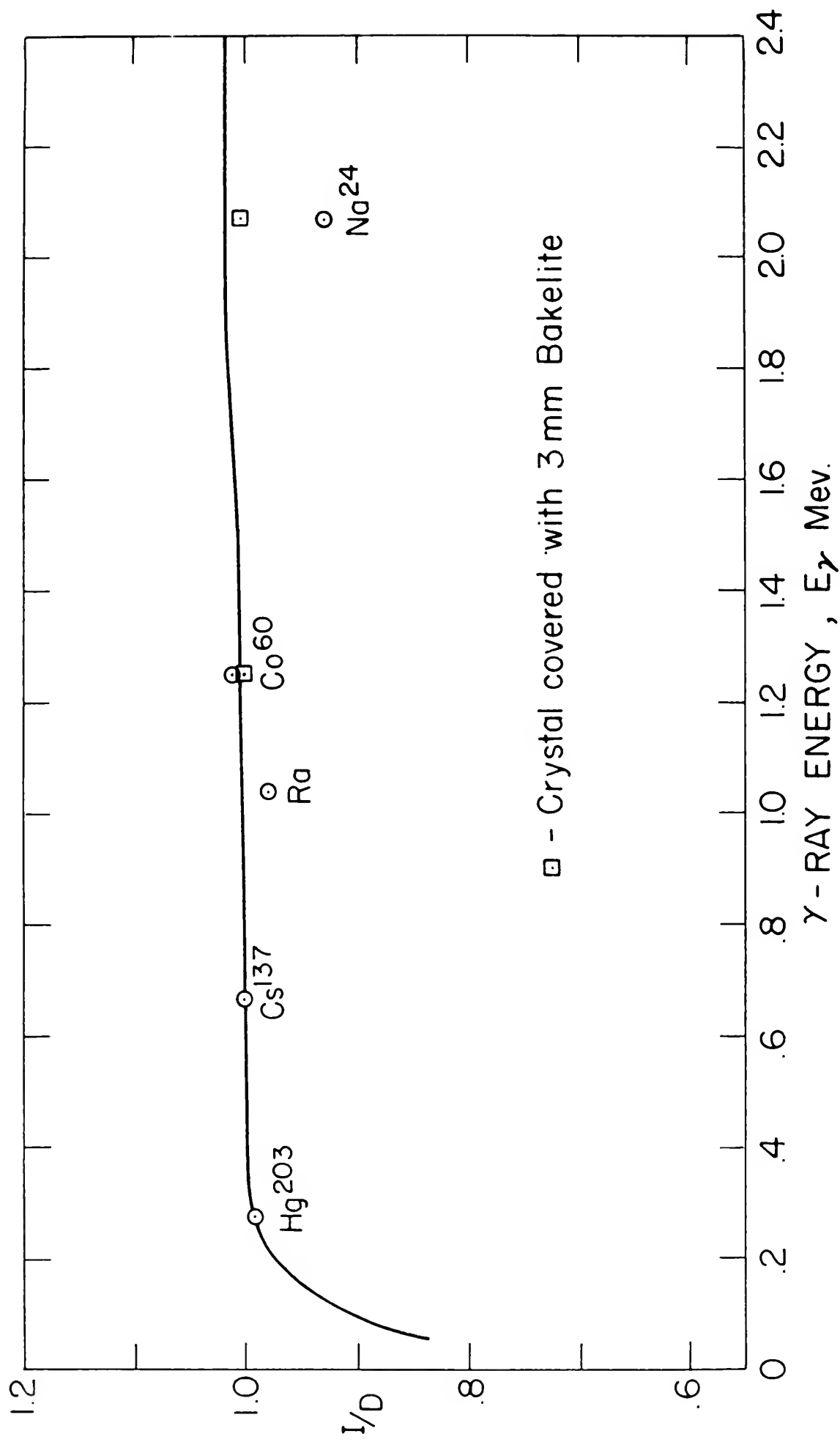
Fig. 6. I/D as a function of  $\gamma$ -ray energy for a 2.5 cm NaI(Tl) crystal. The theoretical curve has been normalized at 1.5 Mev. The experimental data obtained with uncollimated  $\gamma$ -ray beams are normalized for the Co<sup>60</sup>  $\gamma$  rays.



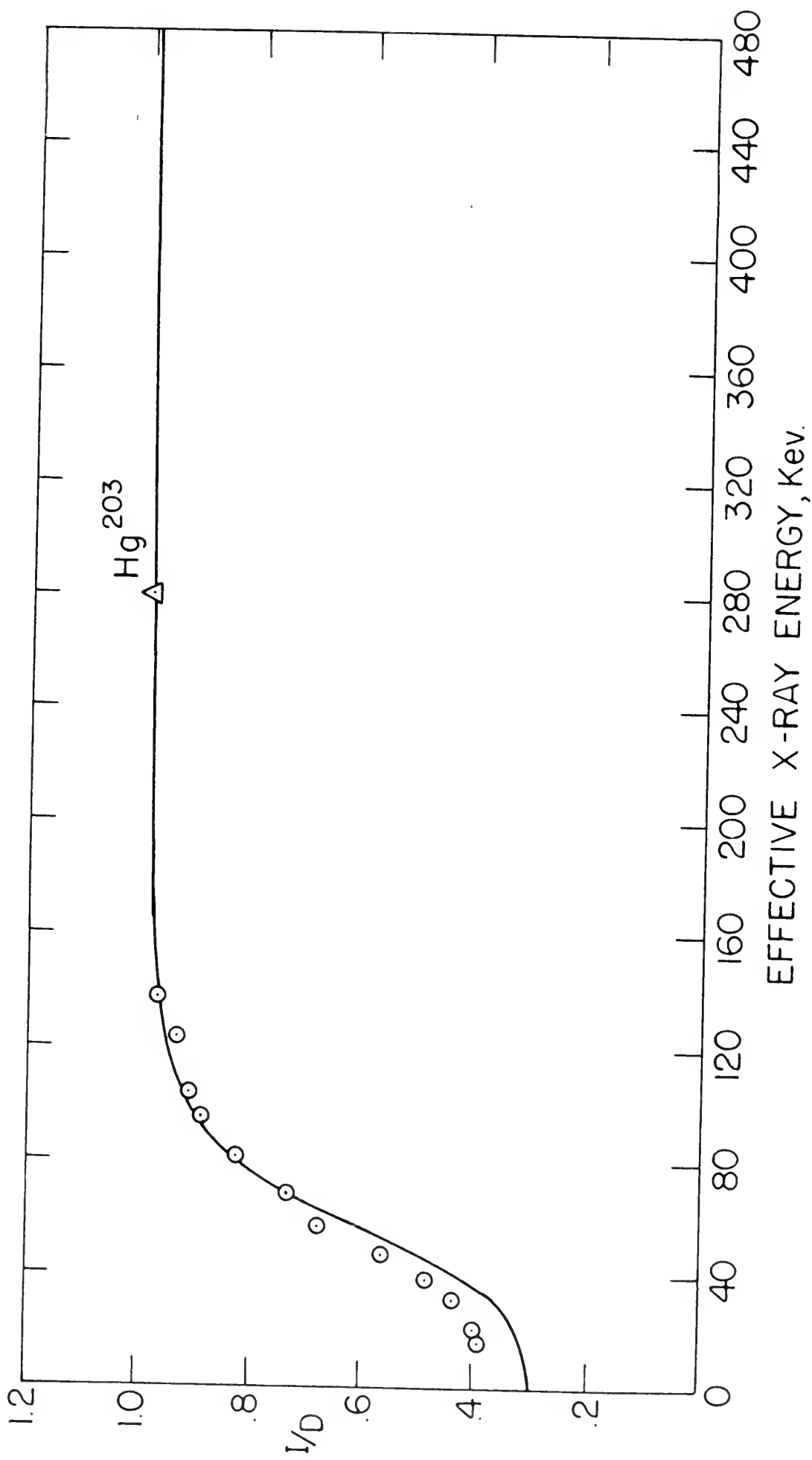




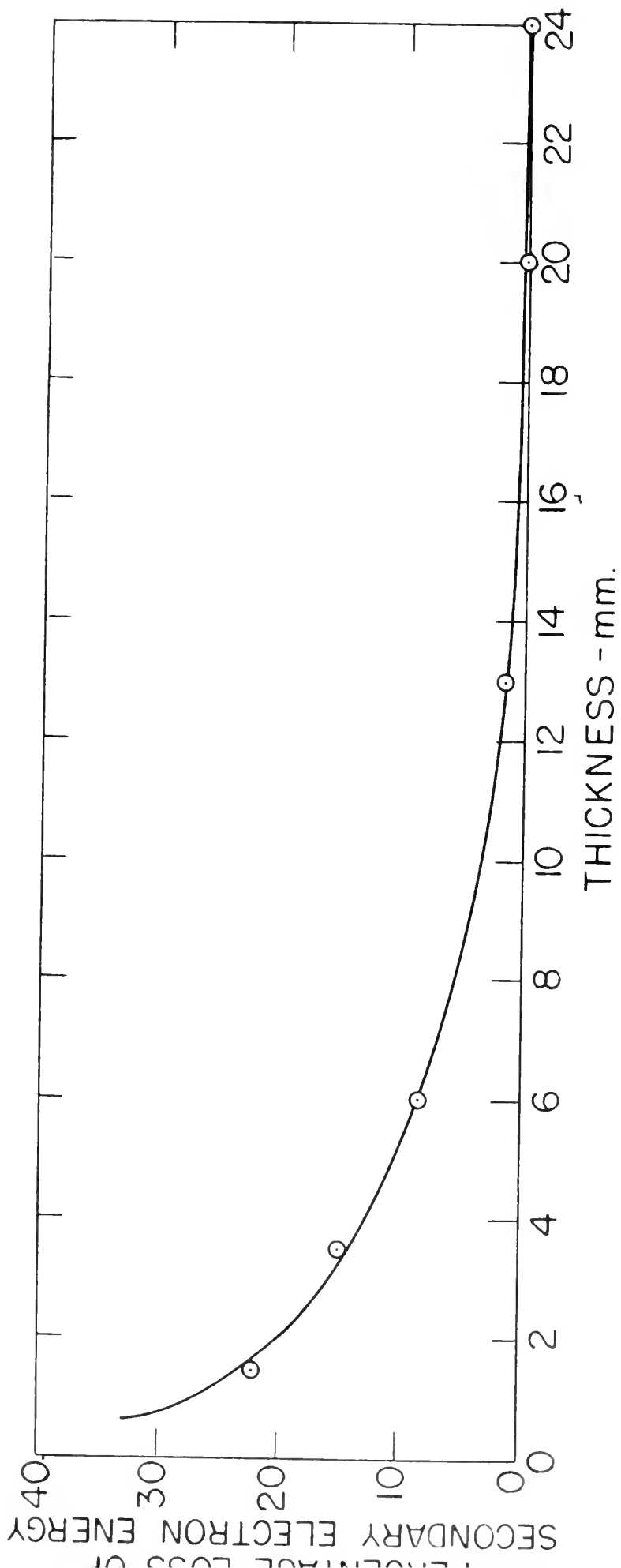




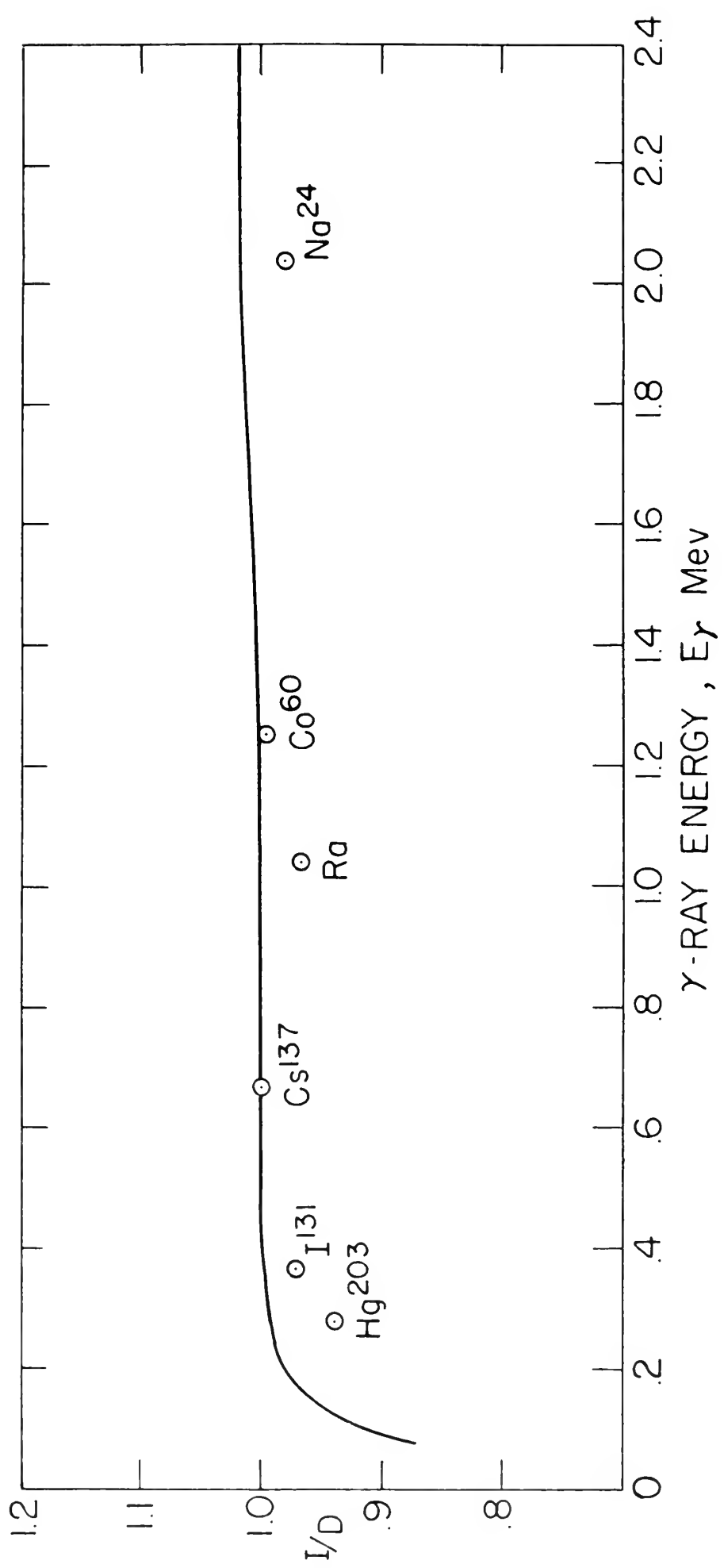






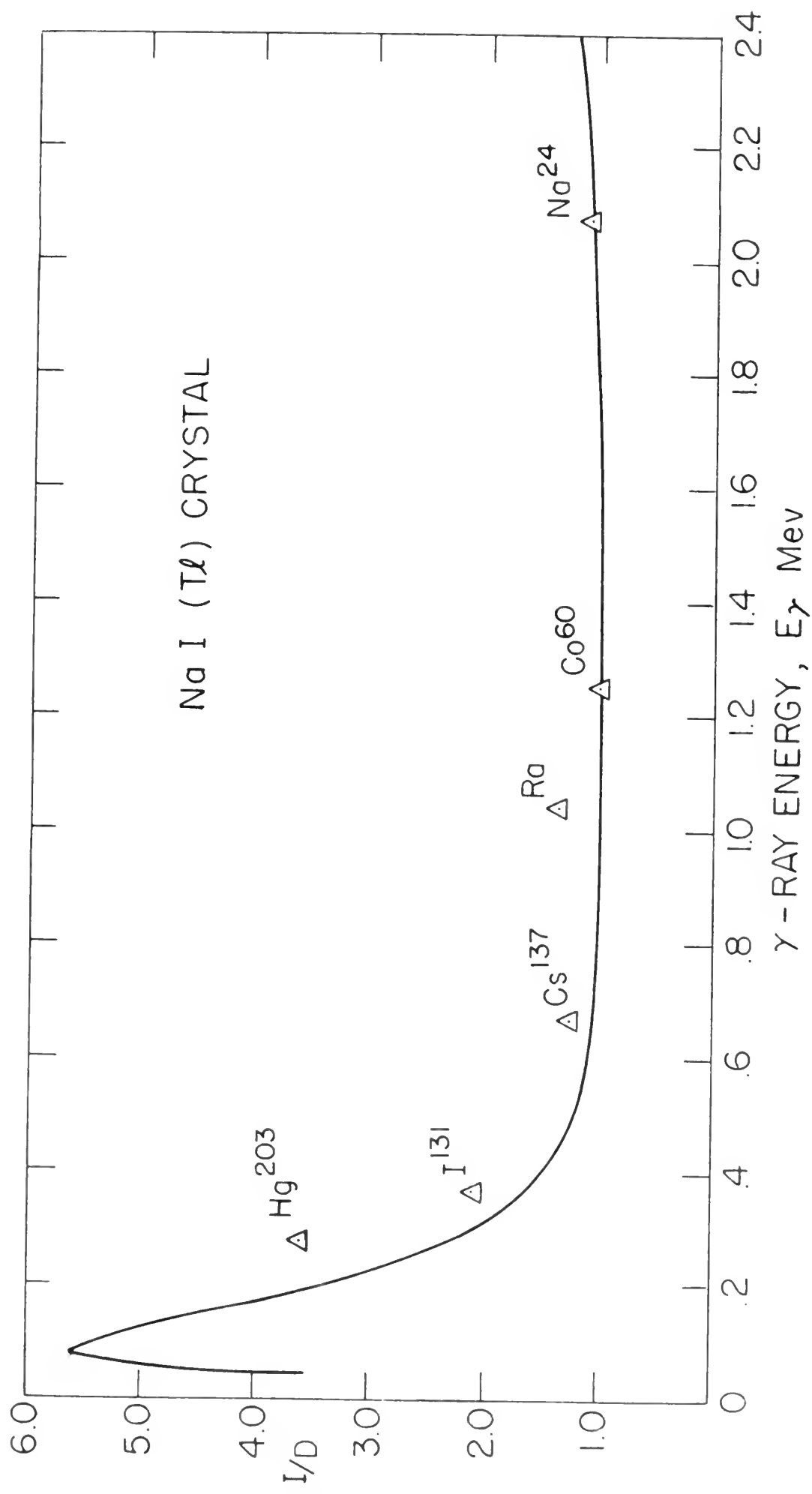














PHOTOMOUNT  
PAMPHLET BINDER

Manufactured by  
GAYLORD BROS. Inc.  
Syracuse, N. Y.  
Stockton, Calif.

JAN 29

AG 664

41861

14384

Thesis Carr

21454

C2716 Physical basis for gamma-ray scintillation dosimetry.

JAN 29

AG 664

41861

14384

21454

Thesis Carr

C2716 Physical basis for gamma-ray scintillation dosimetry.

thesC2716  
Physical basis for gamma-ray scintillati



3 2768 002 09240 5  
DUDLEY KNOX LIBRARY